Solubility of Lithium Salts Formed on the Lithium-Ion Battery Negative Electrode Surface in Organic Solvents

Journal of The Electrochemical Society, **156** (12) A1019-A1027 (2009)
0013-4651/2009/156(12)/A1019/9/$25.00 © The Electrochemical Society

Solubility of Lithium Salts Formed on the Lithium-Ion Battery Negative Electrode Surface in Organic Solvents

Ken Tasaki,[a,*,z] Alex Goldberg,[b] Jian-Jie Lian,[b] Merry Walker,[c,d] Adam Timmons,[c] and Stephen J. Harris[c,*]

[a]*Mitsubishi Chemical USA, Redondo Beach, California 90277, USA*
[b]*Accelrys Software, Incorporated, San Diego, California 92121, USA*
[c]*General Motors Research and Development Center, Warren, Michigan 48090, USA*
[d]*University of Michigan, Ann Arbor, Michigan 48502, USA*

The solubility of lithium salts in dimethyl carbonate (DMC) found in solid electrolyte interface (SEI) films was determined. The salt–DMC solutions evaporated, and the salts were transferred into water for ion conductivity measurements. The salts examined included lithium carbonate (Li_2CO_3), lithium oxalate [$(LiCO_2)_2$], lithium fluoride (LiF), lithium hydroxide (LiOH), lithium methyl carbonate ($LiOCO_2CH_3$), and lithium ethyl carbonate ($LiOCO_2C_2H_5$). The salt molarity in DMC ranged from 9.6×10^{-4} mol L^{-1} ($LiOCO_2CH_3$) to 9×10^{-5} mol L^{-1} (Li_2CO_3) in the order of $LiOCO_2CH_3 > LiOCO_2C_2H_5 > LiOH > LiF > (LiCO_2)_2 > Li_2CO_3$. X-ray photoelectron spectroscopy measurements on SEI films on the surface of the negative electrode taken from a commercial battery after soaking in DMC for 1 h suggested that the films can dissolve. Separately, the heat of dissolution of the salts was calculated from computer simulations for the same salts, including lithium oxide (Li_2O), lithium methoxide ($LiOCH_3$), and dilithium ethylene glycol dicarbonate [$(CH_2OCO_2Li)_2$:LiEDC] in both DMC and ethylene carbonate (EC). The results from the computer simulations suggested that the order in which the salt was likely to dissolve in both DMC and EC was $LiEDC > LiOCO_2CH_3 > LiOH > LiOCO_2C_2H_5 > LiOCH_3 > LiF > (LiCO_2)_2 > Li_2CO_3 > Li_2O$. This order agreed with the experiment in DMC within the experimental error. Both experiment and computer simulations showed that the organic salts are more likely to dissolve in DMC than the inorganic salts. The calculations also predicted that the salts dissolve more likely in EC than in DMC in general. Moreover, the results from the study were used to discuss the capacity fading mechanism during the storage of lithium-ion batteries.
 [DOI: 10.1149/1.3239850]

Manuscript submitted May 18, 2009; revised manuscript received July 27, 2009. Published October 9, 2009.

The solid electrolyte interface (SEI) film formed on the electrode in lithium-ion battery cells is believed to be one of the most critical factors that determine battery performance, and it has been the subject of intense research efforts in the past.[1-35] An SEI film affects battery performance characteristics such as the self-discharge, the cycle life, the safety, the shelf life, and the irreversible capacity. Yet, the nature of the SEI film, such as the film formation mechanism, composition, and film characteristics, is still little understood. In this report, we focus on materials that form SEI films on the active material surface of negative electrodes.

Among the important battery performance factors, the lifetime of lithium-ion batteries is increasingly a matter of concern as the market introductions of automobiles equipped with lithium-ion batteries near. It is believed that SEI film characteristics such as their mechanical and thermodynamics properties govern the lifetime to a significant extent.[1] During cycling, the electrode undergoes volume expansions and contractions, which may result in fractures of SEI films. Dissolution of the film may expose the electrode surface to the electrolyte, prompting reactions with the electrolyte that reduce the cell capacity.[4,34,35] It has long been known that lithium-ion batteries suffer a capacity loss during storage.[2] Jean et al. found that the SEI film formed on carbon-based negative electrodes was not stable when stored in contact with electrolytes, promoting self-discharge.[3] Vetter et al. proposed that cell aging stemmed from an increased degradation of SEI films as the film started to break down or to dissolve in the electrolyte.[4] Furthermore, Du Pasquier et al. reported that a peak identified as the decomposition of SEI components in differential scanning calorimetry (DSC) measurements disappeared after rinsing the negative electrode with dimethyl carbonate (DMC), suggesting that they were soluble in DMC.[5] Safari et al. developed an aging model for lithium-ion batteries based on solvent decompositions as the source of capacity fading, simulating various battery aging profiles.[6] Most previous modeling works are also based on similar mechanisms: solvent decompositions[7,8] or continuous SEI film formations.[9] Indeed, Geniès et al. observed an increased resistance from the SEI after the storage of a cell for 6 weeks.[10] This observation suggests changes in SEI film characteristics during storage. Apparently, capacity fading during aging results, at least in part, from the dissolution of the SEI film components in the electrolyte followed by continuous decomposition reactions of the electrolyte, leading to further SEI film formation. Here, we focus on the dissolution of SEI film components, which are largely made of lithium salts.

Recently, Abraham et al. found that when a degraded negative cell was disassembled and the negative electrode was rinsed in the DMC, the cell capacity recovered to a point comparable to the capacity measured during the cell's initial cycles.[11] Likewise, Broussely et al. reported that negative electrodes dismantled after more than 1 year of storage under a charged state at 60°C, but once rinsed with water, demonstrated an ability to cycle lithium at the same initial specific capacity and polarization.[12] These previous findings not only provide important information on the SEI film–solvent interactions, but may also suggest a method by which the faded capacity of a lithium-ion battery can be recovered. Yet, no detailed study of the solubility of the individual SEI components into an electrolyte solvent has been reported except for a computational study.[36] Previous discussions on SEI film dissolutions were based on indirect observations such as the changes in peaks of X-ray photoelectron spectroscopy (XPS) or DSC measurements.[5,13] The objective of this study is to examine the solubility of a series of SEI film components. The lithium salts studied here included lithium fluoride (LiF), lithium hydroxide (LiOH), lithium carbonate (Li_2CO_3), lithium oxalate [$(LiCO_2)_2$], lithium methyl carbonate ($LiOCO_2CH_3$), and lithium ethyl carbonate ($LiOCO_2C_2H_5$). Their solubility was measured in DMC. Because the characteristics of SEI films, including their compositions, vary depending on the active materials and the electrolyte, it is our hope that measurements of the solubility of individual lithium salts would apply to a wide range of SEI film compositions. Computational tools were used not only to interpret the experimental data, but also to supplement the data by analyzing other salts such as lithium oxide (Li_2O), lithium methoxide ($LiOCH_3$), and dilithium ethylene glycol dicarbonate [$(CH_2OCO_2Li)_2$, to be referred to as LiEDC]. The heat of dissolution for each salt in DMC was calculated by molecular dynamics

* Electrochemical Society Active Member.
z E-mail: ken_tasaki@m-chem.com

(MD) simulations and was compared with the experimental results from the solubility measurements where possible. The heat of dissolution for each salt in ethylene carbonate (EC) was also calculated for comparison.

All of the lithium salts studied here have been experimentally observed, and the reactions to produce the salts have been proposed.[1,5,14-35] The reactions associated with the production of lithium salts are summarized below,[1,5,14-35] where $LiPF_6$ is used as the initial lithium salt

$$LiPF_6 \rightarrow LiF + PF_5 \quad [1]$$

$$LiPF_6 + H_2O \rightarrow LiF + POF_3 + 2HF \quad [2]$$

$$(CH_2O)_2C=O + 2Li^+ + 2e^- \rightarrow Li_2CO_3 + CH_2=CH_2 \quad [3]$$

$$Li_2CO_3 + LiPF_6 \rightarrow 3LiF + POF_3 + CO_2 \quad [4]$$

$$Li_2CO_3 + 2HF \rightarrow 2LiF + CO_2 + H_2O \quad [5]$$

$$2CO_2 + 2Li^+ + 2e^- \rightarrow Li_2CO_3 + CO \quad [6]$$

$$H_2O + Li^+ + e^- \rightarrow LiOH + \tfrac{1}{2}H_2 \quad [7]$$

$$LiOH + Li^+ + e^- \rightarrow Li_2O + \tfrac{1}{2}H_2 \quad [8]$$

$$Li_2CO_3 + PF_5 \rightarrow 2LiF + POF_3 + CO_2 \quad [9]$$

$$ROCO_2R + Li^+ + e^- \rightarrow LiOCO_2R + \tfrac{1}{2}R_2 \quad [10]$$

$$2LiOCO_2R + H_2O \rightarrow Li_2CO_3 + 2ROH + CO_2 \quad [11]$$

$$ROCO_2R + 2Li^+ + 2e^- \rightarrow Li_2CO_3 + R_2 \quad [12]$$

$$LiOCO_2R + HF \rightarrow LiF + ROH + CO_2 \quad [13]$$

$$ROCO_2R + 2Li^+ + 2e^- \rightarrow 2LiOR + CO \quad [14]$$

$$2(CH_2O)_2C=O + 2Li^+ + 2e^- \rightarrow (CH_2OCO_2Li)_2 + CH_2=CH_2 \quad [15]$$

$$(CH_2OCO_2Li)_2 \rightarrow Li_2CO_3 + CH_2=CH_2 + CO_2 + \tfrac{1}{2}O_2 \quad [16]$$

$$Li_2CO_3 \rightarrow Li_2O + CO_2 \quad [17]$$

$$O_2 + 4Li^+ + 4e^- \rightarrow 2Li_2O \quad [18]$$

$$(CH_2OCO_2Li)_2 + 2Li^+ + 2e^- \rightarrow (LiCO_2)_2 + (CH_2OLi)_2 \quad [19]$$

$$2CH_3OCO_2Li + 2Li^+ + 2e^- \rightarrow (LiCO_2)_2 + 2LiOCH_3 \quad [20]$$

where R is either CH_3 or C_2H_5; thus, R_2 can be either C_2H_6 or C_4H_{10}, respectively. As can be seen in the above reactions, some lithium salts are products of direct reductions of organic solvents, while the others are decomposition products, often further consuming lithium. Some reactions produce water, which can set off additional salt decomposition steps. Many of the above reactions are interdependent, mostly in equilibrium. This suggests a complex series of cascading reactions at the SEI during storage. We attempt to address the role of the salt dissolution in the SEI film formation reactions and the SEI film components and the compositions as a whole.

Experimental

LiF, Li_2CO_3, $Li_2C_2O_4$, and LiOH were purchased from Aldrich, while $LiOCO_2CH_3$ and $LiOCO_2C_2H_5$ were purchased from Organomed (Coventry, RI), which synthesized them according to the procedure of Dedryvère et al.[37] DMC was purchased from Ferro Corp. (Cleveland, OH). The chemicals were used as received. Initially, we attempted to measure the solubility of the salts by dissolving them in DMC and measuring the Li concentration with an inductively coupled plasma (ICP) or with flame ionization. However, a weak Ar line that overlapped the Li line in the ICP interfered with the ICP measurement, while the flame ionization measurements were not sufficiently reproducible. Instead, solubilities of the salts in DMC were determined by measuring ion conductivities using a temperature-compensated Oakton Acorn CON-6 conductivity meter from Oakton Instruments (Vernon Hills, IL). This device is designed for water solutions, not DMC solutions, so we followed the following procedure. All chemical operations were carried out in a glove box filled with high quality Ar gas. Excess salt was put in a 10 mL vial that was then filled with DMC. The vial was sealed, removed from the globe box, and shaken for 10 h at ambient temperature under ambient pressure to ensure that the salt–DMC solution was saturated. Shaking the vial was extended to 1 week, but no difference in the final results was observed. The vial was transferred back into the glove box where it was unsealed. The supernatant liquid was then drawn through a 2 μm filter, trapping any undissolved salt. The saturated solution that passed through the filter was left to evaporate, leaving behind the salt that had been dissolved. This recovered salt was then removed from the glove box and dissolved in a measured volume of distilled and deionized water, in which all of the salts were highly soluble. The concentration of the salt was determined by measuring the ionic conductivity of the salt aqueous solution and comparing that result to a set of calibration curves. The calibration curves were generated by dissolving a known mass of the same salt into distilled and deionized water and measuring the resulting conductivity. We then successively diluted the salt aqueous solution by factors of 2 until the conductivity meter reading was about 1 $\mu S\ cm^{-1}$, near the lower limit for the meter. We repeated three measurements for each salt to present the mean solubility and one standard deviation from the mean. The temperature was maintained at 25°C during the measurements. The concentration in water was then converted to the original concentration in DMC. Measurements for Li_2O and $LiOCH_3$ could not be carried out because they reacted chemically with water. To examine a possibility that highly soluble impurities in the salts could have been responsible for the conductivity signals, separate experiments were run. First, each salt was presoaked and shaken in excess DMC for about 10 h. The supernatant liquid with possible impurities was then discarded, and the remaining undissolved salt was used for the solubility measurements according to the above procedure. The results with and without the presoaking procedure agreed to within experimental error.

XPS is a common tool for the electrode surface chemistry analysis; yet, the findings vary among research groups.[21,26,35,38-41] It is plausible that *ex situ* electrode treatments before examination such as rinsing with a solvent may have altered the surface characteristics in some cases. Therefore, we examined negative electrode surfaces before and after soaking for 1 h in DMC to search for this effect. To avoid using a laboratory-specific SEI film, we examined negative electrodes taken out of a disassembled LM40 laptop battery pack manufactured by LGChem, model LR1865AH without any surface pretreatment. Details of the material components used in the cell are not known though we suspect that the artificial graphite was used for the negative electrode. After being fully charged, the battery cell was disassembled in a globe box under Ar atmosphere to extract the negative electrode. It was carried under argon to a Kratos Axis Ultra spectrometer with a monochromatized Al Kα radiation ($h\nu$ = 1486 eV). The spectrometer was calibrated using the photoemission line Ag $3d_{5/2}$. The core spectra were recorded with a 20 eV constant pass energy. No charge neutralization was used. Peak assignments were made according to the previous studies.[34] We repeated this procedure several times starting from different batteries and analyzed representative spectra. All measurements were conducted at ambient temperature.

Computational

The lithium salt examined by computational simulations included, in addition to the salts subjected to the experimental mea-

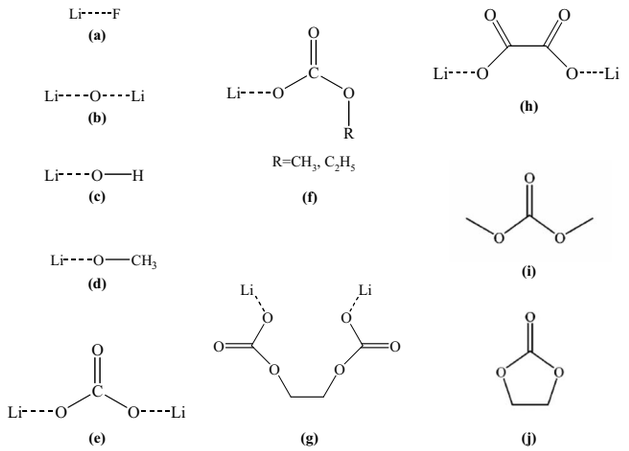

Figure 1. The chemical structures of all molecules studied: (a) lithium fluoride, (b) lithium oxide, (c) lithium hydroxide, (d) lithium methoxide, (e) lithium carbonate, (f) lithium methyl (R = CH_3) or ethyl cabonate (R = C_2H_5), (g) dilithium ethylene glycol dicarbonate, (h) lithium oxalate, (i) DMC, and (j) EC.

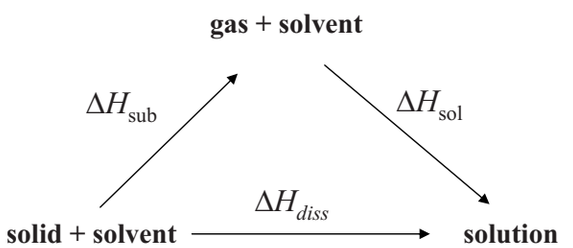

Figure 2. The thermodynamic cycle used for the calculations of the heat of sublimation (ΔH_{sub}), the heat of solution (ΔH_{sol}), and the heat of dissolution (ΔH_{diss}).

surements mentioned above, Li_2O, $LiOCH_3$, and LiEDC. Figure 1 shows the chemical structures of all molecules involved in the calculations. Figure 2 illustrates the thermodynamic cycle used in the calculations of the heat of dissolution for each salt in DMC and EC. The heat of sublimation (ΔH_{sub}), the heat of solution (ΔH_{sol}), and the heat of dissolution (ΔH_{diss}) were obtained from the following equations

$$\Delta H_{sub} = \Delta E_{sub} + RT \quad [21]$$

$$\Delta H_{sol} = \Delta E_{sol} - RT \quad [22]$$

$$\Delta H_{diss} = \Delta H_{sub} + \Delta H_{sol} \quad [23]$$

where ΔH_{sub} is the energy required to bring the salt from the condensed phase to the gas phase and ΔE_{sol} is the energy required to transfer the same salt from the gas phase to the organic solvent.[42,43] Both ΔE_{sub} and ΔE_{sol} are the potential energies obtained from the MD simulations. R and T are the gas constant and the absolute temperature, respectively. The temperature was 25°C. The volume change between the salt solution and the liquid (DMC or EC) in the calculation of the heat of solution was assumed negligible.[43]

The heat of dissolution predicted by MD simulations largely depends on the quality of the force field. The force field used to calculate the potential energy needed for an evaluation of the intra- and intermolecular interactions for individual molecules was COMPASS, including automatic parameters developed by Accelrys, Inc., except for the atomic charges.[44-46] The atomic charges were derived from density functional theory (DFT) calculations using the Perdew–Burke–Ernzerhof exchange-correlation functional[47,48] through the electrostatic potential fitting. The basis set was the double-numerical polarization basis set including one atomic orbital (AO) for each occupied AO, the second set of valence AOs, d-functions for non-hydrogen atoms, and p-functions on hydrogen atoms.[49] The atomic charges thus derived for each salt and solvent are shown in Fig. 3. For each salt, 1 ns simulations were run under the *NPT* ensemble, under which the number of atoms, the pressure, and the temperature were constant during the simulation, for a cell having a side length of roughly 20 Å. The exception was LiEDC,

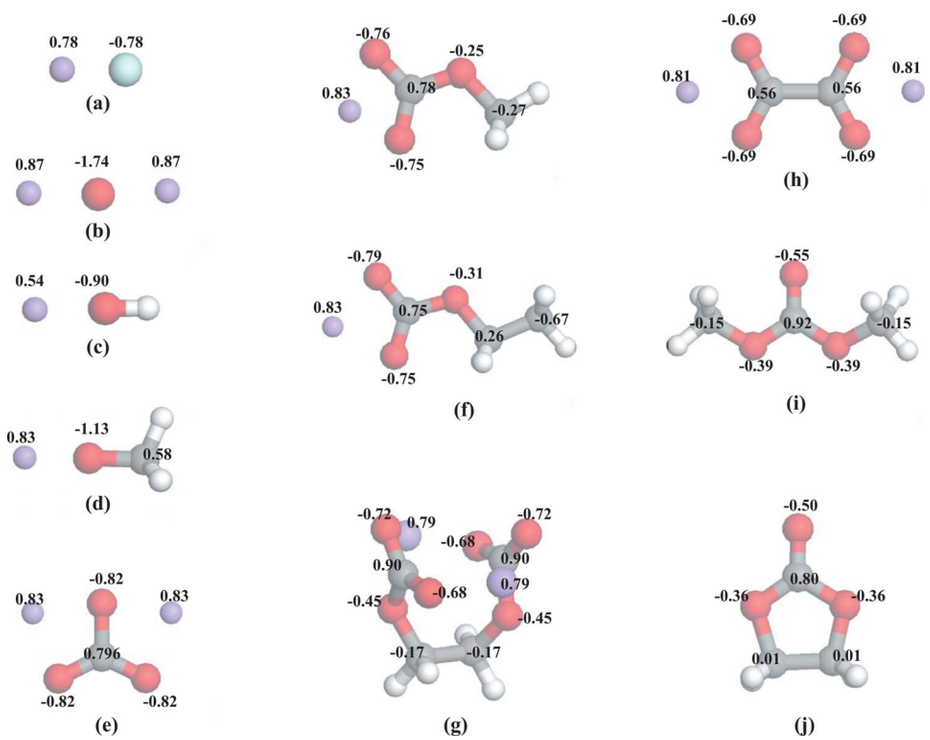

Figure 3. (Color online) The atomic charges for the salts, not shown for the hydrogen atoms, used in computer modeling. (a)–(j) show the same molecules as those in Fig. 1. The structures displayed were taken from the optimized structures by energy minimization by DFT calculations. See the text for details.

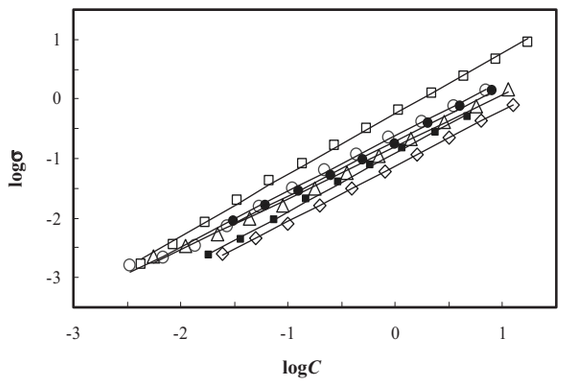

Figure 4. The calibration curves used for the determination of the salt concentration in water: LiOH (□), Li_2CO_3 (○), LiF (●), $(LiCO_2)_2$ (△), $LiC_2H_5CO_3$ (■), and $LiCH_3CO_3$ (◇). The logarithm of the ion conductivity was plotted against the logarithm of the salt concentration for each salt. The unit for the conductivity was mS cm^{-1}. The unit for the concentration was mg salt per 20 mL water. All the measurements were conducted at 25°C.

which required longer simulations, 2 ns, especially in solid, due to its larger molecular size. The average value from several runs was taken for the potential energy used for the heat calculations. The long range interactions, both van der Waals and electrostatic interactions, were treated by the Ewald summation.[50] The crystal structures were used for the solids when the crystallographic data were available. For LiOH,[51] LiF,[52] $(LiCO_2)_2$,[53] Li_2CO_3,[54] and Li_2O,[55] the crystal structure was used, while amorphous structures were generated for the others using the Amorphous Cell software package.[46]

Results and Discussion

Figure 4 shows a log–log plot of the calibration curves for each salt in water used to determine the salt concentration from the ion conductivity measurements. The average slope for all of the curves was 0.95 ± 0.06, which is close to the expected value of 1. The observed linear relationship between the logarithm of the ion conductivity and the logarithm of the salt concentration may be consistent with a well-known relationship between the ion conductivity and the concentration

$$\sigma = N_A e z C u \quad [24]$$

where σ is the conductivity of the salt in water, N_A is the Avogadro number, e is the electron charge, z is the charge number of the salt ion, C is the concentration of the salt, and u is the mobility of the salt in water. Assuming that u is constant over a wide range of C, a linear relationship with a slope of 1 between log σ and log C is expected. The concentration obtained from the curve was then converted to the original concentration in DMC.

Table I summarizes the results from the solubility measurements for the salts in DMC. In the table, the solubility is expressed in terms of both ppm (mass/mass) and molarity M (mol L^{-1}) of each salt in DMC. It is well accepted that the solubility of a solute in a solvent is related to the similarity between their molecular structures.[56] As expected, the two organic salts, $LiOCO_2CH_3$ and $LiOCO_2C_2H_5$, dissolved more than other salts. The former was more soluble than the latter in DMC because of the closer structural similarity of the former to DMC than the latter. The dilithium salts, Li_2CO_3 and $(LiCO_2)_2$, were the least soluble among them. The salts were likely to dissolve in the order of $LiOCO_2CH_3$ > $LiOCO_2C_2H_5$ > LiOH > LiF > $(LiCO_2)_2$ > Li_2CO_3 in terms of M. Assuming that a salt constitutes 10% of a 50 nm thick SEI film having a total of 1 cm^2 of surface area, a somewhat arbitrary assumption, the volume of pure DMC required to dissolve Li_2CO_3 is only 77.5 μL. This simple estimate is consistent to the finding by Abraham et al.[11] and Du Pasquier et al.,[5] though the individual components in the SEI film were not reported in their work. Still, the above estimate is based on a very rough assumption. Kang et al.[57] and West et al.[58] suggested that the SEI can also be induced to dissolve via an electrochemical process.

Though the above experiment dealt with the solubility of individual salts separately, the solubility of a full SEI film in pure solvents can also be observed. Figure 5 illustrates the XPS spectra for the negative electrode taken from a commercial battery before and after soaking in the solvents. Given the little information on the active material for the electrode and the electrolyte used in the battery cell, the discussion is limited to a qualitative interpretation. The four core peaks are shown in the figure: Li 1s, C 1s, F 1s, and O 1s. The peaks taken before (the broken line) and after soaking in DMC (the solid line) highlight a sharp contrast on the electrode surface characteristics. The spectra, in general, exhibit a reduced intensity after soaking in DMC except for the C 1s spectrum. This observation suggests considerable changes in the electrode surface chemistry, presumably dissolution of the SEI film components into DMC. The spectra for the electrode before soaking confirm the presence of lithium salts such as LiF at 685 eV in the F 1s spectrum and at 56 eV in the Li 1s spectrum,[13] Li_2CO_3 at 55.5 eV in the Li 1s spectrum and at 533 eV in the O 1s spectrum,[34] and organic salts at around 531 eV in the O 1s spectrum.[34] After soaking in DMC, the C 1s peak at around 285 eV, due to the graphite carbon, was enhanced, suggesting that the SEI film dissolution exposed the graphite surface. The increased peaks both around 290 eV in the C 1s spectrum and around 687 eV in the F 1s spectrum after soaking may be due to the salts that resided in the lower SEI layer before soaking and appeared after the upper SEI layer was removed by dissolution in DMC. The former peak position is close to that of Li_2CO_3, while the latter resembles that of $LiPF_6$ though it is possible that the peak is due to the binder poly(vinylidene difluoride). These results are consistent with the report by Andersson and Edsröm.[34] Lu et al. attributed the change in the negative electrode surface chemistry during storage to the decomposition of the original salts except for the lithium sulfates.[38] Our intention here is not to quantitatively compare the solubility of individual salts with the XPS data but rather to examine the relevance of our solubility measurements for the individual lithium salts as the SEI film components. The electrode examined here was soaked in pure DMC; thus, the result does not reflect exact conditions in a real cell.

Table II lists the heat of dissolution for each salt obtained from MD simulations, along with the heat of sublimation and the heat of solution in DMC and EC. LiEDC has a large exothermic heat of dissolution, while $LiOCO_2CH_3$ shows a moderately exothermic heat. Our previous work predicted the heat of dissolution for LiEDC

Table I. The solubility of various lithium salts in DMC. The measurements were conducted at 25°C.

	Li_2CO_3	$(LiCO_2)_2$	LiF	LiOH	$LiOCO_2C_2H_5$	$LiOCO_2CH_3$
ppm[a]	6 ± 1	9 ± 5	4 ± 1	14 ± 8	47 ± 9	73 ± 30
M [b] (mol L^{-1}) $\times 10^4$	0.9 ± 0.2	1.0 ± 0.5	1.7 ± 0.4	6.8 ± 3.6	5.3 ± 1.0	9.6 ± 3.9

[a] Parts per million in mass/mass.
[b] Salt molarity.

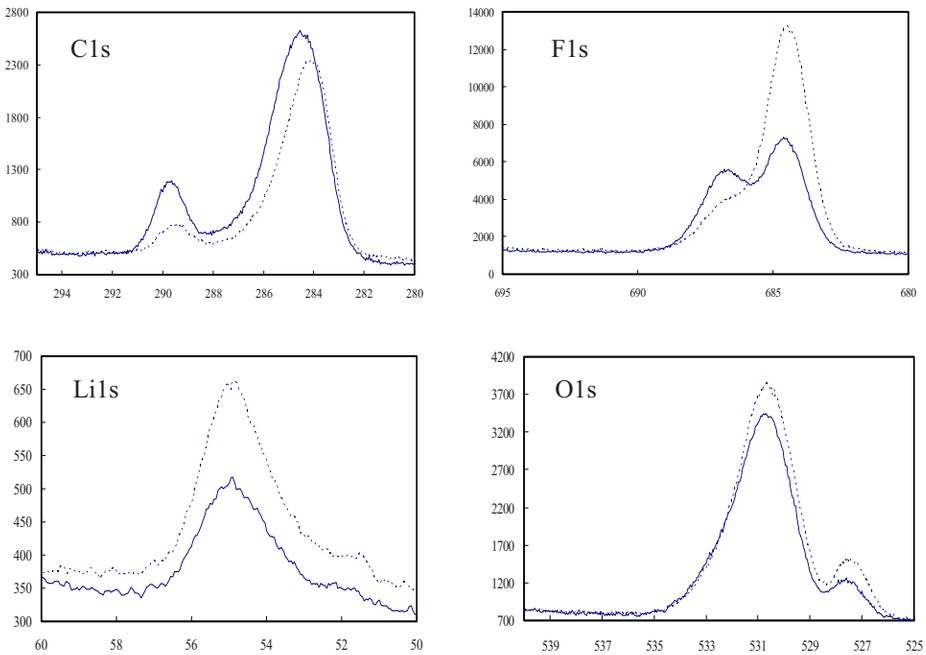

Figure 5. (Color online) C 1s, F 1s, Li 1s, and O 1s XPS spectra for the negative electrode before soaking (the broken line) and after soaking (the solid line) in DMC for 1 h at room temperature.

to be endothermic.[36] However, the force field used in the previous work was different from the current one and never compared against any experimental data. The heat of dissolution for the rest is either exothermic or endothermic, depending on the salt or the solvent. The salts tend to dissolve somewhat more in EC than in DMC, in general, due to the higher polarity of EC than DMC. The order in which the heat of dissolution becomes more endothermic in DMC coincides well with the order of solubility in terms of the molarity obtained from the experiment, at least for those for which the experimental data were obtained. An exception is LiOH, which is predicted to be more soluble than $LiOCO_2C_2H_5$ though a qualitative agreement is still met within the experimental errors, as shown below.

Figure 6 plots the ratio of the molarity in the natural logarithmic scale ($\ln(M_1/M_n)$) against the difference in the heat of dissolution between the salts divided by $RT(-[\Delta H_{diss}(1) - \Delta H_{diss}(n)]/RT)$, where 1 and n refer to $LiOCO_2CH_3$ and any other salt, respectively. $\ln(M_1/M_n)$ is expressed by a bar including the experimental errors in the figure. The relative positions of $-[\Delta H_{diss}(1) - \Delta H_{diss}(n)]/RT$ with the statistical errors shown by the horizontal line fall within the experimental errors of the corresponding $\ln(M_1/M_n)$, demonstrating the relative solubility of the experimental data reasonably reproduced by the calculations. Both experiments and calculations show Li_2CO_3 as the least soluble salt in DMC. A thin film of sputtered Li_2CO_3 has been used as a passivation film on the negative electrode surface to prevent electrolyte decompositions.[58]

Crystal structures were not used for all the salts in the simulations because crystallographic data were available only for LiOH, LiF, $(LiCO_2)_2$, Li_2CO_3, and Li_2O. Instead, amorphous structure forms were used for other salts. The effect of not using a crystal structure on the heat of dissolution was examined for those salts for which the crystal structure is known. For amorphous simulations, to avoid having a system stuck in a shallow potential energy well, the cell was first heated to 600 K and then gradually cooled to 298 K; this was followed by a 1–2 ns simulation at the same temperature. For LiOH, LiF, $(LiCO_2)_2$, Li_2CO_3, and Li_2O, the values of the heat of dissolution obtained from such amorphous simulations were 1.24, 7.45, 8.49, 23.94, and 80.02 kcal mol^{-1}, respectively. The differences from those obtained from the crystal simulations ranged from 0.14 kcal mol^{-1} for LiOH to 37.38 kcal mol^{-1} for Li_2O. Yet, the order in the heat of dissolution either in DMC or EC was not altered. Some studies have found amorphous regions in SEI films.[13]

Experimental data for a direct comparison to the calculations are limited. Table III summarizes the comparison with the available literature values, the heat of vaporization for DMC [59] and EC,[60] and

Table II. The heat of sublimation, the heat of solution, and the heat of dissolution for various lithium salts (kcal mol^{-1}) (obtained as average over 1 ns MD simulations at 25°C).

	Li_2O [a]	Li_2CO_3 [a]	$(LiCO_2)_2$ [a]	LiF[a]	$LiOCH_3$	LiOH[a]	$LiOCO_2C_2H_5$	$LiOCO_2CH_3$	LiEDC
					In DMC				
ΔH_{sub}	98.97	79.57	83.01	62.26	50.47	95.50	52.24	49.02	148.40
ΔH_{sol}	−55.72	−66.05	−71.26	−51.74	−45.94	−93.82	−50.44	−52.38	−169.46
ΔH_{diss}	42.66	12.93	11.16	9.92	3.94	1.10	1.21	−3.95	−21.65
					In EC				
ΔH_{sub}	98.97	79.57	83.01	62.26	50.47	95.50	52.24	49.02	148.40
ΔH_{sol}	−55.59	−58.49	−76.44	−53.81	−52.06	−95.23	−56.63	−53.68	−161.85
ΔH_{diss}	42.79	20.49	5.98	7.86	−2.18	−0.313	−4.99	−5.25	−14.04

[a] The crystal structure was used for the simulations. See Ref. 51-55.

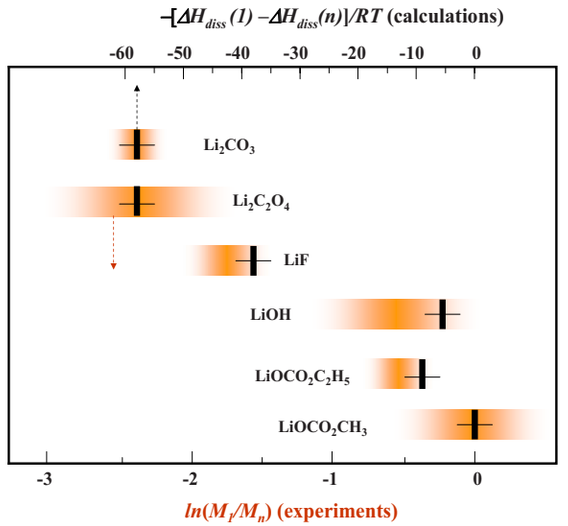

Figure 6. (Color online) The natural logarithm of M_1/M_n, $\ln(M_1/M_n)$, the lower axis, plotted against $-[\Delta H_{diss}/(1) - \Delta H_{diss}/(n)]/RT$, the upper axis, for the salts where 1 refers to $LiOCO_2CH_3$ while n refers to any other salt. The wide bar represents $\ln(M_1/M_n)$ with the experimental error, while the perpendicular line shows $-[\Delta H_{diss}/(1) - \Delta H_{diss}/(n)]/RT$, with the statistical error shown by a thin horizontal line.

also the heat of sublimation for LiF,[61] all of which are reasonably reproduced by the calculations. One can argue that the errors associated with both the heat of sublimation and the heat of solution by our calculations may be canceled out because the heat of dissolution is a summation of ΔH_{sub} and ΔH_{sol}. However, the comparison of ΔH_{sub} with the experimental data does not support the claim, at least for LiF. Still, the calculations are only meant to be compared to the experiments qualitatively because they only give the heat of dissolution and the entropy is difficult to calculate for the systems studied. We believe, however, that the relative discussion among the salts studied is still relevant, judging from the plots in Fig. 4.

Lithium diffusion in each salt solid was also examined using the results from computer simulations. The self-diffusion coefficient, D, of the lithium ion can be calculated by the following equation

$$D = \lim_{t\to\infty} \frac{\langle |r(t) - r(0)|^2 \rangle}{6t} \quad [25]$$

where $|r(t) - r(0)|^2$ is the mean-square displacement of the lithium ion, with $r(t)$ and $r(0)$ being its position at time = t and 0, respectively, obtained from the trajectory of the simulations. The bracket denotes an ensemble average from the simulations. Table IV indicates the self-diffusion constant for each salt in solid thus obtained. The calculated values vary widely among the salts, with the organic salts having higher diffusion constants and with the inorganic salts having much lower constants in general. The difference largely stems from the amorphous and the crystal structures used for simulations. Yet, the values should not be taken as quantitative, given the only qualitative agreement obtained for the calculations with respect to the solubility data.

Our results show that the organic lithium salts of an SEI film are more likely to dissolve in the electrolyte than the inorganic salts though the Li^+ concentration in the electrolyte affects the solubility of the lithium salts as the SEI film components in the electrolyte. Among the salts, LiEDC has the largest exothermic heat of dissolution. Organic salts can be the majority of the SEI components from solvent reductions,[32] LiEDC having been reported as the major component of SEI films,[14,15,34] and their layers are often positioned above the inorganic components.[62,63] Andersson and Edsröm also reported based on XPS measurements that LiEDC was removed from the electrode surface in a cell stored after 7 days,[34] without identifying the cause.

Based on our results, combined with previous studies on reactions of lithium salts and organic solvents, we will speculate as to what happens to the SEI film during storage. The organic lithium salts of the SEI film may dissolve into the electrolyte in the beginning of storage, depending on their solubility. Because the inorganic salts often form a particulate morphology, as has been reported,[32,34] exposing the active negative electrode surface, they promote reductions of the organic solvent along with further consumption of lithium. The exposed surface is prone to the reactions with the electrolyte to form more SEI films, consuming more lithium.[4,34,35] Because the major component, LiEDC, possesses two lithium ions per molecule, its high solubility only accelerates the lithium consumption. This process of the organic lithium salts being dissolved into the electrolyte and their redeposition on the exposed active material surface may be repeated as long as there are reactants to be consumed and enough kinetic energy is available. Such a process of SEI film dissolution and redeposition during electrode cycling has been previously discussed.[13]

Table III. Comparisons of calculations and experimental data. The experimental data are in the parentheses. The temperatures measured and calculated for DMC, EC, and LiF were 25, 150, and 25°C, respectively.

	DMC	EC	LiF
Heat of vaporization, kcal mol^{-1}	9.47 ± 0.48 (9.26[a])	12.04 ± 0.42 (13.45[b])	—
Heat of sublimation, kcal mol^{-1}	—	—	62.26 (64.59[c])

[a] Reference 59.
[b] Reference 60.
[c] Reference 61.

Table IV. The self-diffusion coefficient for the lithium salt solid (obtained from mean-square displacements of the lithium ion calculated from MD simulations performed at 25°C, according to Eq. 25).

	Li_2O [a]	Li_2CO_3 [a]	$(LiCO_2)_2$ [a]	LiF[a]	$LiOCH_3$	LiOH[a]	$LiOCO_2C_2H_5$	$LiOCO_2CH_3$	LiEDC
$D \times 10^7$ cm^2 s^{-1}	1.6×10^{-5}	9.0×10^{-4}	4.6×10^{-3}	3.5×10^{-5}	1.1	1.3×10^{-3}	0.3	0.7	0.8

[a] The crystal structure was used for the simulations. See the text for the references.

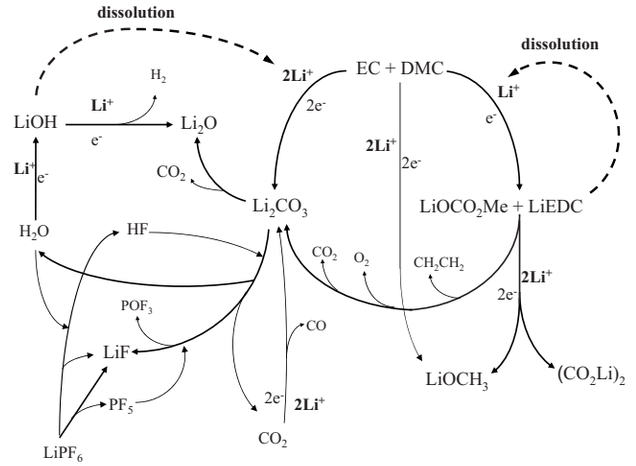

Figure 7. Reactions associated with the formation of SEI films, the decompositions, and the dissolution of the salts, possibly occurring during storage, illustrating progressive lithium consumptions by the reactions when $LiPF_6$ was used as the lithium salt and EC and DMC were used as the organic solvents. All the reactions were taken from literatures,[1,5,14-35] though not all of Eq. 1-20 could be included due to the space limitation. Some by-products are also not shown for clarity.

We also speculate that the new SEI film formed during storage may be different from that before storage because some of the SEI lithium salts studied here can be produced by a decomposition of the other salts. For example, Li_2CO_3 is decomposed to yield Li_2O.[19] Furthermore, Zhuang and Ross proposed that lithium oxalate found in an SEI film may be formed by a decomposition of lithium alkyl carbonate,[20] which has been confirmed by another group.[21] It has been proposed that LiEDC can be decomposed into Li_2CO_3 as well.[30] During storage or cycling, some components studied here may become more predominant than others, which makes the solubility of an SEI film as a whole more complex.

Figure 7 summarizes the reactions comprising some of Eq. 1-20, which may occur at the active material surface or in the SEI film during the first charge cycle and the subsequent storage. Not all equations are included due to the space limitation. Figure 7 is not intended to accurately describe the reactions in the SEI film. Rather, Fig. 7 is to illustrate schematically the cascading reactions of lithium salts set off by the reduction reactions of the electrolyte while consuming more lithium ions, going further down the successive reactions. Most of the cascading lithium salt reactions end at LiF, Li_2O, and $(LiCO_2)_2$, with many reactions leading to LiF. LiF crystallites have been found on the graphite surface in the $LiPF_6$ electrolyte after storage.[34]

In the absence of these decomposition reactions of lithium salts, the lithium ions would be simply recycled through the dissolution of lithium salts into the electrolyte, and capacity loss would not occur through this mechanism. Likewise, without dissolution of the salts into the electrolyte, the succession of salt decompositions would eventually come to cease, as the availability of reactants becomes less, thus reducing the rate of capacity fading. Yet, the capacity fade rate does not decline and may even grow in some cases during storage[8,10] though a loss of integrity of the cells is a possibility.[12] Furthermore, the growth of SEI films has also been observed by XPS, scanning electron microscopy analysis, and other means.[8,10,34,38] We propose that it is the dissolution of some of the salts and the subsequent reduction of the electrolyte that drive the cascade decomposition reactions to a significant degree by supplying the reactants for the salt decompositions, consuming lithium continuously, and contributing to more SEI film growth.

During storage, the reduction reactions may produce more organic salts under a very low current,[62] which further promotes dissolution into the electrolyte, triggering more reactions with the electrolyte. It follows that during storage, the SEI film undergoes cycles of dissolution into the electrolyte and formation of the film on the graphite surface through further reactions with the electrolyte. In the meantime, the decomposition reactions from the lithium salts to other salts continue, giving rise to progressively more inorganic components such as LiF, Li_2CO_3, and Li_2O, including an organic salt such as $(LiCO_2)_2$, all of which are less soluble in the organic solvents.

Figure 8 illustrates a hypothetical evolution in the SEI film composition during storage, showing only a few cycles of dissolution, reduction, and decomposition–redeposition of the SEI film components. The organic components should also include the polymeric phase, which is a part of the SEI film,[1,34] but the discussion of the polymer phase is beyond the scope of this paper. As the composition of the SEI film becomes more inorganic, the diffusion of lithium ions through the film may be more hindered, as the results in Table IV suggest. The increased impedance from the SEI during aging has been reported.[10] This model, however, is not meant to describe anything on the film thickness, but rather on the film composition.

Because the SEI film is likely to be phase-separated between the crystal and the amorphous phases and also because it undergoes a continuous transformation of the compositions through salt dissolutions, reductions, and decompositions, the film may lack a fundamental thermodynamic stability. Cohen et al. suggested that SEI components are in a state of dynamic equilibrium with constant changes in the SEI morphology caused by dynamic dissolution and precipitation of its constituents.[64] Still, our discussion is entirely based on the solubility results of the lithium salts and therefore should be taken only as a speculation. Though our model is consistent with previous findings,[8-10,34,38,64,65] further detailed study is warranted. Also, the capacity fading mechanism discussed here is

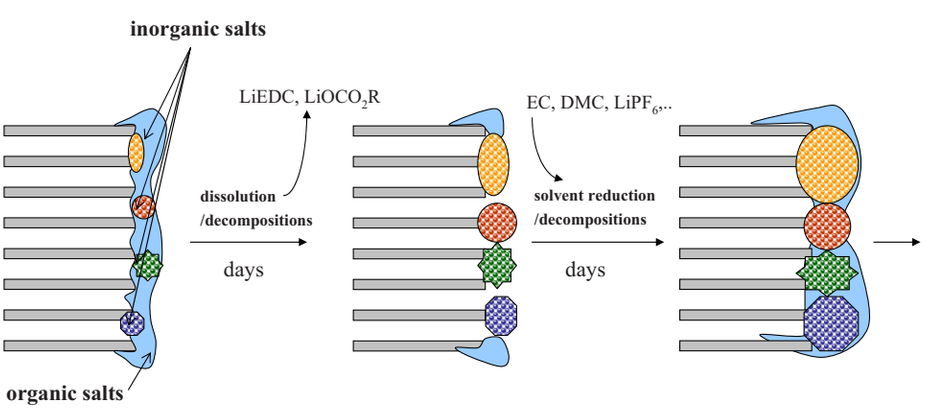

Figure 8. (Color online) A hypothetical representation of the SEI film compositional change through cycles of dissolutions and decompositions of salts and solvent reductions during storage. The far right figure does not necessarily represent the composition at the end of storage. The outer layer of the SEI film on the edge side of graphite may have the organic components, including LiEDC, $LiOCO_2R$, and some polymeric materials, among others. The inorganic components are shown by particle-like domains, including LiF, Li_2CO_3, Li_2O, and others. The composition of the inorganic salts depends on the cell conditions.

only based on the SEI characteristics on the anode side. The impedance of the SEI on the cathode increases during storage.[66]

Conclusion

The solubility of lithium salts, which are well-known individual SEI components, has been determined in DMC through ion conductivity measurements. Among the salts studied here, the order in which the salt was likely to dissolve was $LiOCO_2CH_3 > LiOCO_2C_2H_5 > LiOH > LiF > (LiCO_2)_2 > Li_2CO_3$. The organic salts were more likely to dissolve than the inorganic salts in DMC. The heat of dissolution for some more salts in DMC and EC was also calculated by computer simulations. The predicted heat of dissolution in DMC and EC became more exothermic in the order of $LiEDC > LiOCO_2CH_3 > LiOH > LiOCO_2C_2H_5 > LiOCH_3 > LiF > (LiCO_2)_2 > Li_2CO_3 > Li_2O$. The relative solubility among the salts examined by experiments was reproduced by our calculations. LiEDC is found to have a particularly large exothermic heat of dissolution in both DMC and EC. Our XPS experiments also showed that the SEI film on the negative electrode surface dissolve in pure DMC within a short period of time.

We speculate that during storage, an SEI film undergoes a cycle of film formation, dissolution, redeposition, and decomposition, which result in a continuing consumption of lithium, thus reducing the capacity further. This cycle also causes a continuous change in the film compositions during storage, affecting the SEI impedance. Further study is required to examine in detail the correlation between the SEI composition and capacity fading. The measurements of the solubility at different temperatures will be the subject of our next report. The combined information from Tables I-III and Fig. 7 may be instructive to design a stable SEI film without a high resistance against the Li^+ transfer. Tables I and II give the solubility data on lithium salts, which determine the SEI film stability during storage, Fig. 7 shows what would possibly remain in the film after storage, and Table IV provides the information on the Li^+ transfer.

Computer modeling of solubility for such a heterogeneous system as the SEI film including organic salts, inorganic salts, and organic solvents is challenging due to the lack of parameters as well as experimental data and has been rarely reported. This work attempts to model the complex nature of SEI film components; yet, the current force field may require further improvements because it has been validated through only a few direct comparisons with experimental data. With an improved force field and additional experimental data, more reliable predictions are possible, for example, for the solubility of SEI components at other temperatures.[10] Such predictions may lead to a better understanding of battery degradation.

Acknowledgments

The authors thank Dr. David Rigby, Dr. Matthew Hat, and Dr. George Fitzgerald of Accelrys Software, Incorporated and Maria Militello and Dr. Ion Halalay of General Motors for their very helpful comments and advice. We acknowledge the arrangement made by Professor Ann Marie Sastry of the University of Michigan for Merry Walker's work at General Motors.

Mitsubishi Chemical USA assisted in meeting the publication costs of this article.

References

1. E. Peled, D. Goloditsky, and D. J. Penciner, in *Handbook of Battery Materials*, J. O. Besenhard, Editor, p. 419, Wiley-VCH, Weinheim (1999).
2. A. Andersson, K. Edström, and J. O. Thomas, *J. Power Sources*, **81-82**, 8 (1999).
3. M. Jean, A. Chausse, and R. Messina, Abstract 146, p. 169, The 192nd Electrochemical Society Meeting Abstracts, Vol. 192, Paris, France, 1997.
4. J. Vetter, P. Novák, M. R. Wagner, C. Veit, K. C. Moller, J. O. Besenhard, M. Winter, M. Wohlfahrt-Mehrens, C. Vogler, and A. Hmmouche, *J. Power Sources*, **147**, 269 (2005).
5. A. Du Pasquier, F. Disma, T. Bowmer, A. S. Gozdz, G. Amatucci, and J.-M. Tarascon, *J. Electrochem. Soc.*, **145**, 472 (1998).
6. M. Safari, M. Morcrette, A. Teyssot, and C. Delacourt, *J. Electrochem. Soc.*, **156**, A145 (2009).
7. R. Darling and J. Newman, *J. Electrochem. Soc.*, **145**, 990 (1998).
8. R. P. Ramasamy, J. W. Lee, and B. N. Popov, *J. Power Sources*, **166**, 266 (2007).
9. P. Ramadass, B. S. Haran, P. M. Gomadam, R. White, and B. N. Popov, *J. Electrochem. Soc.*, **151**, A196 (2004).
10. S. Geniès, D. Brun-Buisson, Y.-F. Wu, F. Mattera, and J. Merten, Abstract 1280, The 214th Electrochemical Society Meeting Abstracts, Vol. 802, Honolulu, 2008.
11. D. P. Abraham, J. L. Knuth, D. W. Dees, I. Bloom, and J. P. Christophersen, *J. Power Sources*, **170**, 465 (2007).
12. M. Broussely, Ph. Biensan, F. Bonhomme, Ph. Blanchard, S. Herreyre, K. Nechev, and R. J. Staniewicz, *J. Power Sources*, **97–98**, 13 (2001).
13. S. Leroy, F. Blanchard, R. Dedryvère, H. Martinez, B. Carre, D. Lemordant, and D. Gonbeau, *Surf. Interface Anal.*, **37**, 773 (2005).
14. D. Aurbach, Y. Ein-Eli, B. Markovsky, A. Zaban, S. Luski, Y. Carmeli, and H. Yamin, *J. Electrochem. Soc.*, **142**, 2882 (1995).
15. D. Aurbach, M. D. Levi, E. Levi, and A. Schechter, *J. Phys. Chem. B*, **101**, 2195 (1997).
16. S. Leroy, F. Blanchard, R. Dedryvère, H. Martinez, B. Carre, D. Lemordant, and D. Gonbeau, *Electrochim. Acta*, **47**, 1423 (2002).
17. A. Augustsson, M. Herstedt, J.-H. Guo, K. Edstrom, G. V. Zhuang, P. N. Ross, Jr., J.-E. Rubensson, and J. Nordgren, *Phys. Chem. Chem. Phys.*, **6**, 4185 (2004).
18. H. Cheng, C. Zhu, M. Lu, and Y. Yang, *J. Power Sources*, **173**, 531 (2007).
19. S. S. Zhang, K. Xu, and T. R. Jow, *Electrochim. Acta*, **51**, 1636 (2006).
20. G. V. Zhuang and P. N. Ross, *Electrochem. Solid-State Lett.*, **6**, A136 (2003).
21. L. Zhao, I. Watanabe, T. Doi, S. Okada, and J. Yamaki, *J. Power Sources*, **161**, 1275 (2006).
22. R. Fong, U. Von Sacken, and J. R. Dahn, *J. Electrochem. Soc.*, **137**, 2009 (1990).
23. D. Aurbach, B. Markovsky, I. Weissman, E. Levi, and Y. Ein-Eli, *Electrochim. Acta*, **45**, 67 (1999).
24. R. Dedryvère, S. Leroy, H. Martinez, F. Blanchard, D. Lemordant, and D. Gonbeau, *J. Phys. Chem. B*, **110**, 12986 (2006).
25. D. Aurbach, E. Zinigrad, Y. Cohen, and H. Teller, *Solid State Ionics*, **148**, 405 (2002).
26. G. V. Zhuang, H. Yang, B. Blizanac, and P. N. Ross, *Electrochem. Solid-State Lett.*, **8**, A441 (2005).
27. R. Naejus, D. Lemordant, R. Coudert, and P. Willimann, *J. Fluorine Chem.*, **90**, 81 (1998).
28. D. Aurbach, A. Zaban, Y. Gofer, Y. Ein-Eli, I. Weissman, O. Chusid, and O. Abramson, *J. Power Sources*, **54**, 76 (1995).
29. Y. Ein-Eli, B. Markovsky, D. Aurbach, Y. Carmeli, H. Yamin, and S. Luski, *Electrochim. Acta*, **39**, 2559 (1994).
30. M. N. Richard and J. R. Dahn, *J. Electrochem. Soc.*, **146**, 2068 (1999).
31. O. (Youngman) Chusid, E. Ein-Eli, D. Aurbach, M. Babai, and Y. Carmeli, *J. Power Sources*, **43**, 47 (1993).
32. H. Ota, Y. Sakata, A. Inoue, and S. Yamaguchi, *J. Electrochem. Soc.*, **151**, A1659 (2004).
33. H. Ota, Y. Sakata, X. Wang, J. Sasahara, and E. Yasikawa, *J. Electrochem. Soc.*, **151**, A437 (2004).
34. A. M. Andersson and K. Edsröm, *J. Electrochem. Soc.*, **148**, A1100 (2001).
35. K. Xu, S. Zhang, and T. R. Jow, *Electrochem. Solid-State Lett.*, **6**, A117 (2003).
36. K. Tasaki, *J. Phys. Chem. B*, **109**, 2920 (2005).
37. R. Dedryvère, L. Gireaud, S. Grungeon, S. Laruelle, J.-M. Tarascon, and D. Gonbeau, *J. Phys. Chem. B*, **109**, 15868 (2005).
38. M. Lu, H. Cheng, and Y. Yang, *Electrochim. Acta*, **53**, 3539 (2008).
39. V. Eshkenazi, E. Peled, L. Burstein, and D. Golodnitsky, *Solid State Ionics*, **170**, 83 (2004).
40. S. Leroy, H. Martinez, R. Dedryvère, D. Lemordant, and D. Gonbeau, *Appl. Surf. Sci.*, **253**, 4895 (2007).
41. S.-B. Lee and S.-I. Pyun, *Carbon*, **40**, 2333 (2002).
42. C. M. Lousada, S. S. Pinto, J. N. C. Lopes, M. F. M. da Piedade, H. P. Diogo, and M. E. M. da Piedade, *J. Phys. Chem. A*, **112**, 2977 (2008).
43. W. L. Jorgensen, R. C. Binning, Jr., W. L. Jorgensen, and J. D. Madura, *J. Am. Chem. Soc.*, **105**, 1407 (1983).
44. H. Sun, *J. Phys. Chem. B*, **102**, 7338 (1998).
45. B. E. Eichinger, D. Rigby, and J. Stein, *Polymer*, **43**, 599 (2002).
46. The software package is available from Accelrys, Inc., 10188 Telesis Ct, San Diego, CA.
47. J. P. Perdew, K. Burke, and M. Ernzerhof, *Phys. Rev. Lett.*, **77**, 3865 (1996).
48. J. P. Perdew, K. Burke, and M. Ernzerhof, *Phys. Rev. Lett.*, **78**, 1396 (1997).
49. S. Sadhukhan, D. Munoz, C. Adamo, and G. E. Scuseria, *Chem. Phys. Lett.*, **306**, 83 (1999).
50. P. Ewald, *Ann. Phys. (Paris)*, **54**, 519 (1918).
51. N. W. Alcock, *Acta Crystallogr., Sect. B: Struct. Crystallogr. Cryst. Chem.*, **B27**, 168 (1971).
52. J. Thewlis, *Acta Crystallogr.*, **8**, 36 (1955).
53. B. F. Pedersen, *Acta Chem. Scand. (1947-1973)*, **23**, 1871 (1969).
54. Y. Idemoto, J. W. Richardson, N. Koura, S. Kohara, and C.-K. Loong, *J. Phys. Chem. Solids*, **59**, 363 (1998).
55. F. A. Shunk, *Consitution of Binary Alloys*, 2nd suppl., McGraw-Hill, New York (1969).
56. D. W. Krevelen, *Properties of Polymers*, 2nd ed., Elsevier, Amterdam (1976).
57. S.-H. Kang, D. P. Abraham, A. Xiao, and B. L. Lucht, *J. Power Sources*, **175**, 526 (2008).
58. W. C. West, J. F. Whitacre, B. V. Ratnakumar, E. Brandon, J. O. Blosiu, and S. Surampudi, Jet Propulsion Laboratory Technical Reports Server, Document ID 20060032390, Jet Propulsion Laboratory, Pasadena, CA (2000).
59. W. V. Steele, R. D. Chirico, S. E. Knipmeyer, and A. Nguyen, *J. Chem. Eng. Data*, **42**, 1008 (1997).
60. C. S. Hong, R. Wakslak, H. Finston, and V. Fried, *J. Chem. Eng. Data*, **27**, 146

(1982).
61. M. W. Chase, Jr., C. A. Davis, J. R. Downy, Jr., D. J. Frurip, R. A. McDonald, and A. N. Syverud, *JANAF Thermochemical Tables*, 3rd ed., National Bureau of Standard, Washington, DC (1985).
62. H. Ota, T. Sato, H. Suzuki, and T. Usami, *J. Power Sources*, **97–98**, 107 (2001).
63. B. L. Lucht, A. Xiao, S.-H. Kang, and D. P. Abraham, Abstract 0729, p. 729, The 214th Electrochemical Society Meeting Abstracts, Vol. 214, Hawaii, 2008.
64. Y. S. Cohen, Y. Cohen, and D. Aurbach, *J. Phys. Chem. B*, **104**, 12282 (2000).
65. L. Larush, E. Zinigrad, Y. Goffer, and D. Aurbach, *Langmuir*, **23**, 12910 (2007).
66. M.-S. Wu and P.-C. J. Chiang, *Electrochim. Acta*, **52**, 3719 (2007).